Reverse engineering control of the relative phase and populations of two-level quantum systems

Felipe Silveira Fagundes and Emanuel Fernandes de Lima *

Departamento de Física, Universidade Federal de São Carlos (UFSCar), São Carlos, São Paulo 13565-905, Brazil

(Received 17 June 2024; accepted 18 July 2024; published 1 August 2024)

We consider the simultaneous control of the relative phase and populations of two-level quantum systems by an external field. We apply a reverse engineering approach, obtaining an analytical expression for the control field depending upon two user-defined functions that dictate the population and the relative phase dynamics. We show that, in general, the prescribed functions for the dynamics cannot be chosen arbitrarily, but still there is plenty of room for choice. We illustrate the reverse engineering technique for several target states using different kinds of functions to specify the system dynamics. We show that by adjusting these dynamical functions, we produce different kinds of control fields. These controls can be easily built, needing, apart from the dynamical function themselves, only their first derivatives. The methodology presented here will certainly find many applications that go beyond simple two-level systems.

DOI: 10.1103/PhysRevA.110.022201

I. INTRODUCTION

The investigation of two-level quantum systems is of fundamental interest for physics [1–4]. Despite their simplicity, two-level systems can represent to a very good approximation diverse practical situations and have proven to be adequate to understand the physics content of a variety of coherent phenomena. For instance, a two-level quantum system that interacts with an external time-dependent field can represent an atom under the action of a laser field [5]. The study of two-level systems is also crucial for the development of new technologies as evidenced by the fact that quantum computing faces this kind of system as the fundamental unit of information, the *qubit* [6–8]. Thus it is not a surprise that the search for analytical solutions of driven two-level systems, which started since the early days of quantum mechanics, remains to the present days: these solutions provide deep understanding of the dynamics and also play an essential role in applications [9–13].

A particularly central problem for most applications is the control of the two-level system, i.e., the search of control fields that can drive the initial state to a desired target state at some finite time [14]. The special case of population inversion, where the population of the levels are swept at the final time, can be achieved by several means, e.g., using π pulses [15,16], chirped pulses [17], or adiabatic passage [18,19], to name a few. A more general approach is provided by the optimal quantum control framework, which allows one to drive any initial state to an arbitrary final state [20–23]. The optimal quantum control equations are usually solved numerically and one is often interested in reaching the desired state regardless of the detailed system dynamics.

In an alternative procedure, often referred to as a reverse engineering technique, the control field is designed to follow a dynamical constraint [24–27]. This methodology is encompassed by quantum tracking control, which seeks to find control fields to drive an expectation value of an observable along a prescribed time-dependent *track* [28–32]. This is performed by inverting the equations of motion in order to solve for the control field. Such an approach avoids iterative optimization and thus can be computationally less demanding, although it suffers from the potential appearance of singularities presented in the inversion of the dynamical equations.

The reverse-engineering control of the population dynamics of two-level systems by a resonant pulse has been proposed in Ref. [33]. In this work, an analytical expression for the control field was obtained as a function of an *a priori* specified population dynamics. Apart from the rotating wave approximation (RWA), the phases of the dynamical coefficients were assumed to be fixed, which restricted the applicability of the deduced formula. This work has been followed by investigations considering a two-level system under the influence of dissipative effects [34–36]. Recently [37], the problem of controlling both the populations and phases of a two-level quantum system has been tackled, extending the formula derived in Ref. [33]. In this approach, two functions are prescribed, one for the population and another for the phase of one of the coefficients of the quantum levels. From an analytical integration, the phase of the remaining coefficient is obtained which results in an analytical formula for the control field. One drawback of this approach is the need of performing an integration analytically, which, even when it is possible, in general yields a quite complicated formula for the control field.

In the present work, we address the problem of the simultaneous control of the population and the relative phase of two-level quantum systems through the reversing engineering technique extending previous results [33,37]. The expression of the control field obtained by inverting the equations of motion depends only on the population, the relative phase, and their time derivatives. As a consequence, the control field is

*Contact author: eflima@ufscar.br

determined by prescribing two functions for each one of these quantities. However, additional constraints also follow from the dynamical equations, which implies that the dynamical functions for the population and relative phase cannot be chosen completely arbitrarily. We show that by appropriately choosing these dynamical functions, we obtain analytical expression for the control field without the need of performing any integration. Several initial and target states are chosen to illustrate the approach.

II. CONTROL FRAMEWORK

We consider a two-level system interacting with a linearly polarized, time-dependent external field acting from an initial time $t = t_0$ to a final time $t = t_f$. This system can model, for instance, a two-level atom interacting with a laser pulse. From the knowledge of the initial conditions, our goal will be to specify the system dynamics until a desired target final state is reached. We remark that the present development follows closely Refs. [33,37], but with some key differences. We denote the ground level by $|g\rangle$, with energy E_g, and the excited level by $|e\rangle$, with energy E_e. In atomic units, we write the corresponding total time-dependent Hamiltonian as

$$H = H_0 - \mu\varepsilon(t)(|g\rangle\langle e| + |e\rangle\langle g|), \tag{1}$$

with H_0 being the unperturbed Hamiltonian of the two-level system,

$$H_0 = E_g|g\rangle\langle g| + E_e|e\rangle\langle e| \tag{2}$$

and μ the projection of the electric dipole moment along the field polarization axis. The time-dependent function $\varepsilon(t)$ stands for the electric field and plays the role of the control function. This external field, assumed to be real and with a carrier frequency ω, can be expressed for convenience as two complex-conjugated parts,

$$\varepsilon(t) = \epsilon(t)\mathrm{e}^{-\mathrm{i}\omega t} + \epsilon^*(t)\mathrm{e}^{\mathrm{i}\omega t}, \tag{3}$$

where the complex function $\epsilon(t)$ ultimately defines the envelope and amplitude of the field and the asterisk denotes the complex conjugate.

The wave function can be written in the basis of the eigenstates of the unperturbed Hamiltonian as

$$|\psi(t)\rangle = C_g(t)\mathrm{e}^{-\mathrm{i}E_g t}|g\rangle + C_e(t)\mathrm{e}^{-\mathrm{i}E_e t}|e\rangle, \tag{4}$$

where the time-dependent coefficients $C_g(t)$ and $C_e(t)$ are the complex amplitudes of the ground and excited levels, respectively, in the interaction picture. Upon substitution of this expansion and Eq. (3) in the time-dependent Schrödinger equation, while invoking the RWA, we obtain the following coupled system of differential equations for the coefficients:

$$\begin{aligned}\dot{C}_g(t) &= \mathrm{i}C_e(t)\mu\epsilon^*(t)\mathrm{e}^{\mathrm{i}(\omega-\omega_0)t},\\ \dot{C}_e(t) &= \mathrm{i}C_g(t)\mu\epsilon(t)\mathrm{e}^{-\mathrm{i}(\omega-\omega_0)t},\end{aligned} \tag{5}$$

where $\omega_0 = E_e - E_g$ is the resonance frequency between the energy levels and the dots denote the time derivative.

We can express each complex coefficient in terms of a time-dependent amplitude and phase,

$$C_j(t) = c_j(t)\mathrm{e}^{\mathrm{i}\phi_j(t)}, \tag{6}$$

with the index j denoting either the level g or e, $c_j(t) = |C_j(t)|$ the absolute value, and $\phi_j(t)$ the phase of the corresponding complex coefficient.

Our goal in the work is to derive control fields that yield a prescribed system dynamics. To this end, we rewrite each one of the Eq. (5) in terms of $\epsilon(t)$ and $\epsilon^*(t)$ using Eq. (6),

$$\begin{aligned}\epsilon^*(t) &= -\frac{\mathrm{i}}{\mu}\frac{\dot{c}_g(t) + \mathrm{i}\dot{\phi}_g(t)c_g(t)}{c_e(t)}\mathrm{e}^{-\mathrm{i}[(\omega-\omega_0)t-\phi(t)]},\\ \epsilon(t) &= -\frac{\mathrm{i}}{\mu}\frac{\dot{c}_e(t) + \mathrm{i}\dot{\phi}_e(t)c_e(t)}{c_g(t)}\mathrm{e}^{\mathrm{i}[(\omega-\omega_0)t-\phi(t)]},\end{aligned} \tag{7}$$

where we have defined the relative phase between the coefficients as $\phi(t) = \phi_g(t) - \phi_e(t)$. Substituting Eq. (7) in Eq. (3) and using the conservation of the norm, $c_g\dot{c}_g = -c_e\dot{c}_e$ yields

$$\begin{aligned}\varepsilon(t) =& -\frac{\mathrm{i}}{\mu}\left[\left(\frac{\dot{c}_g(t)}{c_e(t)} + \frac{\mathrm{i}\dot{\phi}_g(t)c_g(t)}{c_e(t)}\right)\mathrm{e}^{\mathrm{i}[\omega_0 t+\phi(t)]}\right.\\ &\left.+\left(-\frac{\dot{c}_g(t)}{c_e(t)} + \frac{\mathrm{i}\dot{\phi}_e(t)c_e(t)}{c_g(t)}\right)\mathrm{e}^{-\mathrm{i}[\omega_0 t+\phi(t)]}\right].\end{aligned} \tag{8}$$

Since we have assumed that the field is a real function, we obtain the following relation among the time derivatives of the phases:

$$\dot{\phi}_e(t) = \frac{c_g(t)^2}{c_e(t)^2}\dot{\phi}_g(t) = \frac{c_g(t)^2}{c_e(t)^2 - c_g(t)^2}\dot{\phi}(t). \tag{9}$$

An important point revealed by the above equation is that when the populations of the levels are equal to each other, the derivative of the relative phase has to vanish.

Equation (9) and the fact that $c_e(t)^2 + c_g(t)^2 = 1$ allow us to write the control field in Eq. (8) as

$$\begin{aligned}\varepsilon(t) =& \frac{2}{\mu}\frac{\dot{c}_g(t)}{|\dot{c}_g(t)|\sqrt{1-c_g(t)^2}}\sqrt{\dot{c}_g(t)^2 + \dot{\phi}_g(t)^2 c_g(t)^2}\\ &\times \sin[\omega_0 t + \phi(t) + \lambda(t)],\end{aligned} \tag{10}$$

where the phase $\lambda(t)$ is given by

$$\lambda(t) = \arctan\frac{\dot{\phi}_g(t)c_g(t)}{\dot{c}_g(t)} = \arctan\frac{1-c_g(t)^2}{1-2c_g(t)^2}\frac{c_g(t)}{\dot{c}_g(t)}\dot{\phi}(t). \tag{11}$$

We are now in a position to apply the reverse engineering idea to our control problem. The dynamical Eq. (5) are to be accompanied by a set of initial conditions specifying the initial populations, $c_g(t_0)^2 \equiv P^i$, $c_e(t_0)^2 = 1 - c_g(t_0)^2$, and the initial phases $\phi_g(t_0)$, $\phi_e(t_0)$ and $\phi(t_0) = \phi_g(t_0) - \phi_e(t_0) \equiv \Phi^i$. From these initial conditions, we set up the population dynamics of the levels and also of the relative phase until they reach the desired target values $c_g(t_f)^2 \equiv P^f$ and $\phi(t_f) \equiv \Phi^f$. To accomplish this task, we define two dynamical functions $P(t)$ and $\Phi(t)$ as

$$\begin{aligned}c_g(t) &= \sqrt{P(t)},\\ \phi(t) &= \Phi(t),\end{aligned} \tag{12}$$

such that they match the initial and final conditions: $P(t_0) = P^i$, $\Phi(t_0) = \Phi^i$, $P(t_f) = P^f$, and $\Phi(t_f) = \Phi^f$.

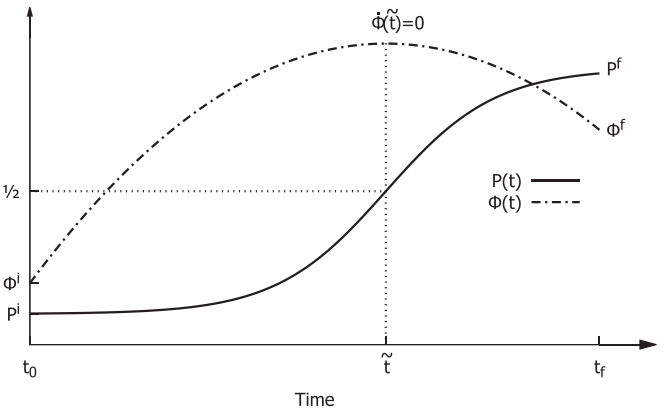

FIG. 1. Schematic drawing of possible dynamical functions $P(t)$ and $\Phi(t)$. The system is driven from $P(t_0) = P^i$ and $\Phi(t_0) = \Phi^i$ to the target values $P(t_f) = P^f$ and $\Phi(t_f) = \Phi^f$. Note that $\Phi(t)$ is chosen such that $\dot{\Phi}(\tilde{t}) = 0$, while $\tilde{t}$ is defined by the condition $P(\tilde{t}) = 1/2$.

From Eq. (10), the engineered external field can be expressed in terms of the dynamical functions $P(t)$ and $\Phi(t)$,

$$\varepsilon(t) = V_0(t)\sin[\omega_0 t + \Phi(t) + \Lambda(t)], \tag{13}$$

where the amplitude and the phase are written as

$$V_0(t) = \frac{2}{\mu}\frac{\dot{P}(t)}{|\dot{P}(t)|}\left[\frac{\dot{P}(t)^2}{4P(t)[1-P(t)]} + \frac{\dot{\Phi}(t)^2 P(t)[1-P(t)]}{[1-2P(t)]^2}\right]^{1/2}, \tag{14}$$

$$\Lambda(t) = \arctan\left[\frac{P(t)[1-P(t)]}{\dot{P}(t)}\frac{2\dot{\Phi}(t)}{1-2P(t)}\right]. \tag{15}$$

Note that there will be no singularity in expression (14) *if* $\dot{\Phi}(t) = 0$ when $P(t) = 1/2$ and $\dot{P}(t) = 0$ in the extrema $P = 1$ and $P = 0$. More formally, we mean that for every $\tilde{t}$ such that $P(\tilde{t}) = 1/2$ the quantity $\dot{\Phi}(t)/[1-2P(t)]$ should be finite in the limit $t \to \tilde{t}$.

Therefore, in the present approach, two dynamical functions $P(t)$ and $\Phi(t)$ are chosen so that they match the initial conditions and reach the desired values of population and relative phase at the final time. The control field that yields the desired dynamics is then given by Eq. (13). However, in addition to the expected smoothness of the dynamical functions, they have to satisfy other constraints: (i) $P(t)$ has to take into account the conservation of the norm $c_g(t)^2 + c_e(t)^2 = 1$, so that $0 \leqslant P(t) \leqslant 1$; (ii) $\dot{P}(t) = 0$ whenever the population reaches an extremum, i.e., $P(t) = 0$ or $P(t) = 1$; (iii) as noticed in Eq. (9), the derivative of the relative phase has to vanish whenever the populations are equal, that is, $\dot{\Phi}(\tilde{t}) = 0$ for all $\tilde{t}$ such that $P(\tilde{t}) = 1/2$; (iv) we must have in mind that we are under the RWA, so that abrupt changes in the functions compared to the system's natural period can break the approximation. Despite these constraints, there is still enough room for choosing the functions to govern the dynamics, as we shall see in the next section.

Figure 1 depicts the possible choice of the dynamical functions $P(t)$ and $\Phi(t)$. In this case, it is intended to drive the system from $P(t_0) = P^i$ and $\Phi(t_0) = \Phi^i$ to the target values of population $P(t_f) = P^f$ and relative phase $\Phi(t_f) = \Phi^f$.

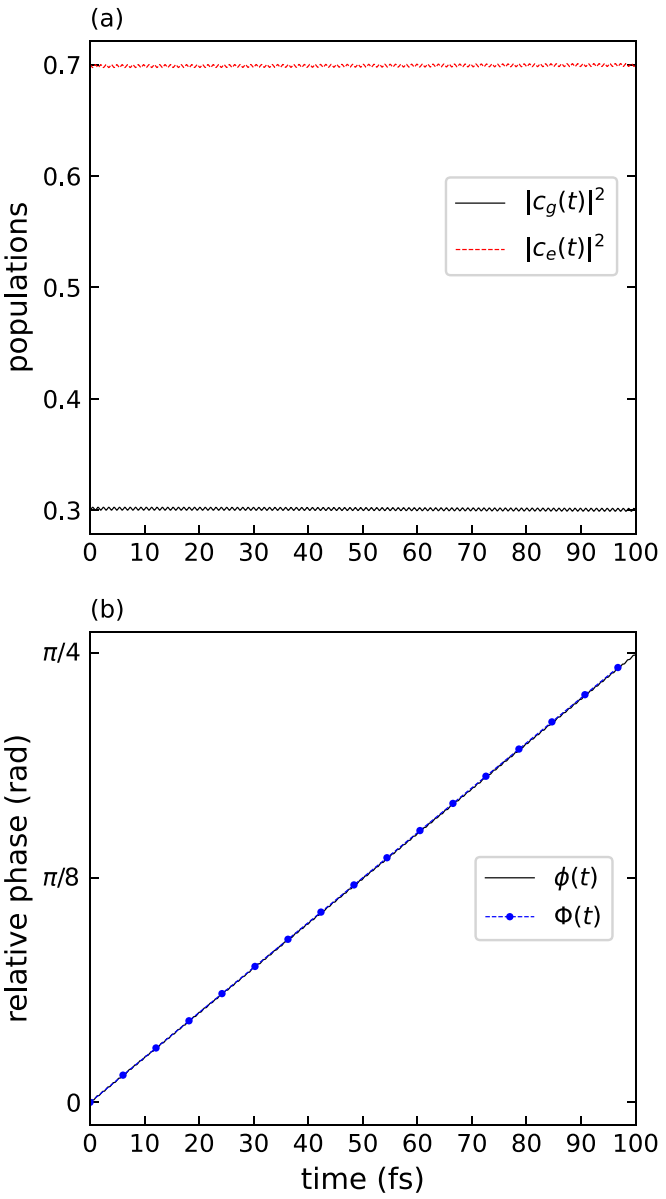

FIG. 2. $P(t)$ is a constant at $P^i = P^f = 0.3$. The initial relative phase is $\Phi^i = 0$ and the target phase is $\Phi^f = \pi/4$. A linear polynomial is chosen for the dynamical function $\Phi(t)$ and formula (17) is used. (a) Levels population dynamics $|c_j(t)|^2$ and (b) relative phase dynamics $\phi(t)$ (continuous line) compared to the chosen dynamics function $\Phi(t)$ (dotted line with points).

The dynamical functions are chosen in order to satisfy the constraints. Especially, the fact that the time derivative of the relative phase is zero when the level populations are equal is highlighted. Note that a myriad of possible functions could be chosen and that the value of $\tilde{t}$ is defined by the selection of $P(t)$.

Finally, it is worth considering two limiting cases. First, if the relative phase is intended to be constant, $\dot{\Phi}(t) = 0$ in the whole interval, and we obtain for the control field

$$\varepsilon_\Phi(t) = \frac{1}{\mu}\frac{\dot{P}(t)}{\sqrt{P(t)[1-P(t)]}}\sin[\omega_0 t + \Phi]. \tag{16}$$

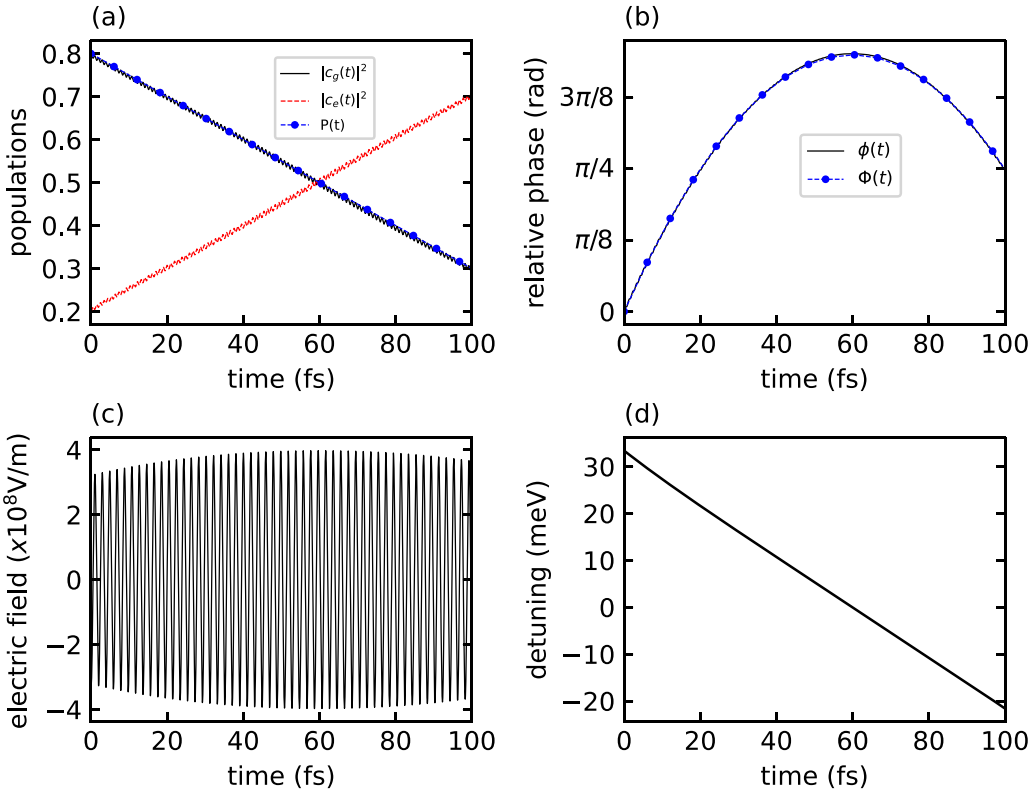

FIG. 3. $P(t)$ is a linear function joining $P^i = 0.8$ to $P^f = 0.3$. The initial relative phase is $\Phi^i = 0$ and the target phase is $\Phi^f = \pi/4$. A quadratic polynomial is chosen for the relative phase such that $\Phi(t_0) = \Phi^i$, $\Phi(t_f) = \Phi^f$, and $\dot{\Phi}(\tilde{t}) = 0$, where $\tilde{t} = 60$ fs. (a) Levels population dynamics along with $P(t)$; (b) relative phase dynamics $\phi(t)$ (continuous line) compared to the chosen dynamics function $\Phi(t)$ (dotted line with points); (c) applied electric field, Eq. (13), and (d) detuning from the resonance frequency $\dot{\Phi}(t) + \dot{\Lambda}(t)$.

Since this result has been explored in previous works, we will not consider this case here [33,38,39].

Now, if it is desired to have the population fixed during the whole interval, the control field can be expressed as

$$\varepsilon_P(t) = \frac{2}{\mu}\frac{\dot{\Phi}(t)\sqrt{P(1-P)}}{1-2P}\cos\left[\omega_0 t + \Phi(t)\right], \qquad (17)$$

with $P(t) = P$ a constant. Note that Eq. (17) will not be useful if $P = 1/2$, because it is not possible to change the relative phase while keeping equal populations; see Eq. (9). In fact, Eq. (17) should be avoided if the population is to be kept too close to $1/2$ due to the small denominator.

III. SIMULTANEOUS CONTROL OF RELATIVE PHASE AND POPULATIONS

Here, we illustrate several cases for the choice of the dynamical functions $P(t)$ and $\Phi(t)$ for different objectives. Following Ref. [37], the parameters of the two level system are chosen to model the $3s \rightarrow 3p$ atomic transition of sodium, for which $\omega_0 = 2.1$ eV and $\mu = 2.479$ atomic units. In all cases, we set $t_0 = 0$. The engineered control field is used to solve numerically the Schrödinger equation without the RWA.

Initially, we consider the situation in which one desires to change only the relative phase, while keeping the populations constants during the whole time interval. We assume the population of the ground level is to be fixed in 0.3 and a change of the relative phase from $\Phi^i = 0$ to $\Phi^f = \pi/4$ is desired, with $t_f = 100$ fs. Thus the function $P(t)$ is just a constant equal to $P^i = P^f = 0.3$ and we chose $\Phi(t)$ as a straight line joining Φ^i and Φ^f. We then apply formula (17) for the control field. Note that, in this case, the control field is a square pulse with constant amplitude of 0.9×10^8 V/m and blueshifted from the resonance frequency ω_0 by 5.17 meV. Figure 2 shows the numerical results obtained. Panel (a) shows that the populations are essentially constants, despite small fast oscillations. The desired relative phase is also reached as shown in panel (b). Similar good results are obtained for different values of the target relative phase, maintaining the other parameters fixed. But for larger values of Φ^f the oscillations in the populations increases. This is expected since the amplitude of the control field depends on $\dot{\Phi}(t)$, so the larger the changes in the relative phase the larger the control field amplitude. However, formula (17) is not practical for the populations close to $1/2$ due to the singularity at $P(t) = 1/2$.

Now consider a linear function for the populations $P(t)$ and a quadratic function for the relative phase $\Phi(t)$. We again set $t_f = 100$ fs. Assume it is desired to drive the population of the ground level from $P^i = 0.8$ to $P^f = 0.3$, while the relative phase should go from $\Phi^i = 0$ to $\Phi^f = \pi/4$. Figure 3 shows the results of applying formula (13) to this case. Note that, since $P(t)$ is a linear function, the time at which $P(t) = 1/2$ is $\tilde{t} = 60$ fs. Thus $\Phi(t)$ is built to match the initial and final phases and also $\dot{\Phi}(\tilde{t}) = 0$. The corresponding results are shown in Fig. 3. In panel (a), apart from small oscillations of the populations, the dynamics follows reasonably well the

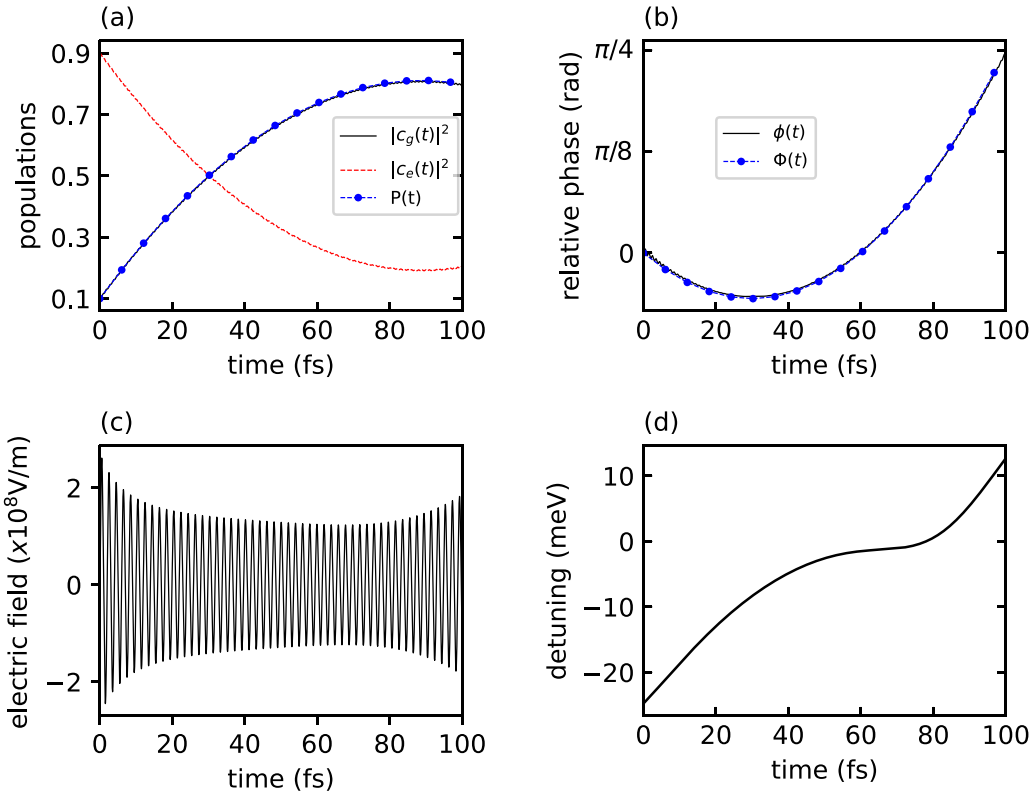

FIG. 4. $P(t)$ is a quadratic polynomial joining $P^i = 0.1$ to $P^f = 0.8$ and such that $P(\tilde{t}) = 1/2$ for $\tilde{t} = 30$ fs. The initial relative phase is $\Phi^i = 0$ and the target phase is $\Phi^f = \pi/4$. A quadratic polynomial is chosen for the relative phase such that $\Phi(t_0) = \Phi^i$, $\Phi(t_f) = \Phi^f$, and $\dot{\Phi}(\tilde{t}) = 0$. (a) Levels population dynamics along with $P(t)$; (b) relative phase dynamics $\phi(t)$ (continuous line) compared to the chosen dynamics function $\Phi(t)$ (dotted line with points); (c) applied electric field, Eq. (13), and (d) detuning from the resonance frequency $\dot{\Phi}(t) + \dot{\Lambda}(t)$.

prescribed linear behavior. The dynamics of the relative phase is quadratic with a maximum at $t = \tilde{t}$ as shown in panel (b). Panel (c) shows that the control field has an almost constant envelope. In panel (d) is shown the detuning $\dot{\Phi}(t) + \dot{\Lambda}(t)$, which represents the instantaneous deviation of the field frequency from ω_0. This panel shows that the control field is essentially a linear chirped pulse. This scheme works satisfactorily for several target values of population and phase. It should be noted, however, that the choice of a linear function for the population dynamics precludes P^i or P^f of being equal to zero or one, because, as already mentioned, $\dot{P}(t)$ should be zero at the extrema. Also note that $\Phi(t)$ cannot be chosen as a quadratic function if $\Phi^i \neq \Phi^f$ and $\tilde{t}$ is exactly in the middle of the time interval, because $\Phi(t)$ could not interpolate the initial and target values while satisfying $\dot{\Phi}(\tilde{t}) = 0$.

Let us examine the choice of $P(t)$ as a quadratic polynomial. Since $P(t)$ has to connect the initial population P^i to the target population P^f, there is an additional point that can be arbitrarily chosen to specify $P(t)$. This extra point may be used to define the value of $\tilde{t}$ for which $P(\tilde{t}) = 1/2$ and $\dot{\Phi}(\tilde{t}) = 0$. Figure 4 shows the results for this case, where $\Phi(t)$ is also a quadratic polynomial $\tilde{t} = 30$ fs and $t_f = 100$ fs. We set $P^i = 0.1$, $P^f = 0.8$, $\Phi^i = 0$, and $\Phi^f = \pi/4$. In panel (a), apart from imperceptible oscillations of the populations, the dynamics follows reasonably the intended quadratic behavior. Panel (b) shows the dynamics of the relative phase with a minimum at $t = \tilde{t}$. Panel (c) shows that the control field decreases its amplitude roughly until $t = 20$ fs, then stays approximately constant up to $t = 80$ fs and increases its amplitude from $t = 80$ fs. Panel (d) shows that the detuning is roughly constant in the interval $t = 50$ fs to $t = 80$ fs and increases approximately linearly from 0 to $t = 50$ fs and from $t = 80$ fs to $t = 100$ fs. This choice for the dynamical functions works very well for several target values of population and phase. However, despite the freedom to set the value of $\tilde{t}$, there is still a drawback if the values of P^i or P^f are either zero or one, as in the previous case, since we cannot generally set $\dot{P}(t) = 0$ at the extrema.

We consider now the choice of $P(t)$ as a hyperbolic tangent function given by

$$P(t) = A \tanh(\alpha t + \beta) + B, \tag{18}$$

where $A = (P^f - P^i)/2$, $B = (P^f + P^i)/2$, and

$$\beta = \frac{1}{2} \ln \frac{1+\gamma}{1-\gamma} - \alpha \tilde{t},$$

where $\gamma = (1/2 - B)/A$. With this setup, $P(t)$ approaches asymptotically the initial and the target values of the populations P^i and P^f, while satisfying $P(\tilde{t}) = 1/2$. As in the case of the quadratic polynomial, the hyperbolic function allows one to tune the value of $\tilde{t}$, but in addition the derivatives of $P(t)$ at the initial and final times can be approximately zero. The parameter $\alpha > 0$ sets how fast the transition rate is between the levels, which occurs around $\tilde{t}$. Figure 5 shows a specific situation, where we have set $P^i = 0.1$, $P^f = 1$, $\Phi^i = 0$, and $\Phi^f = \pi/2$. Once again, $t_f = 100$ fs. Additionally, we have

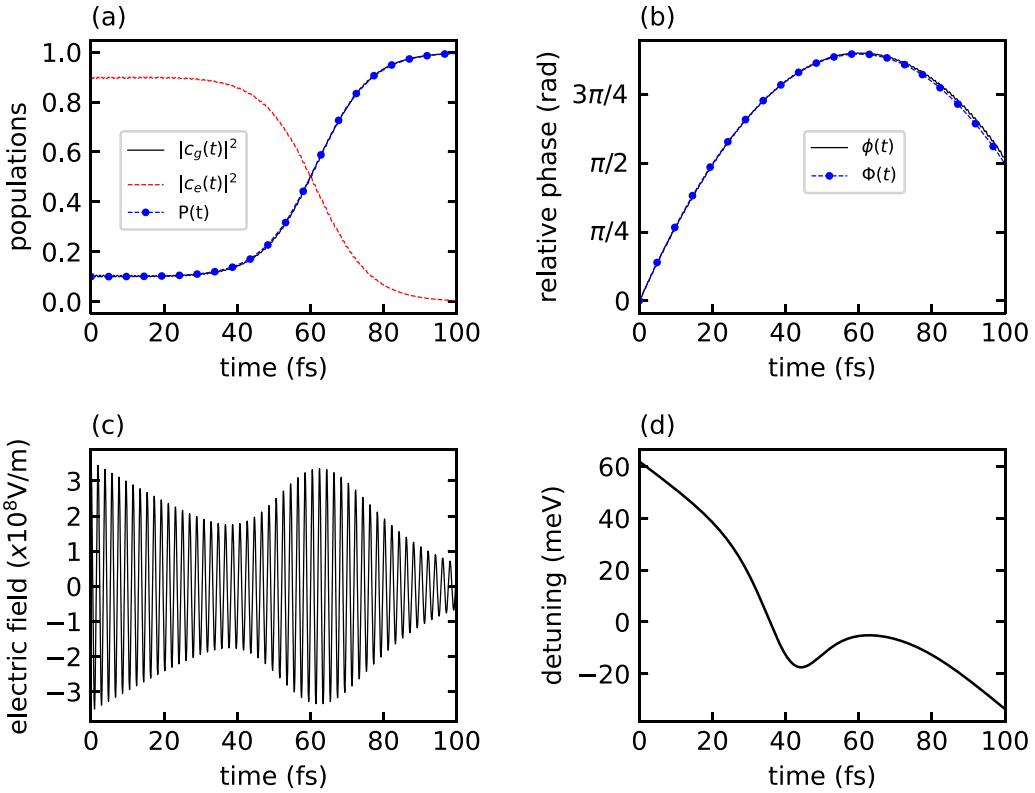

FIG. 5. $P(t)$ is a hyperbolic tangent joining asymptotically $P^i = 0.1$ to $P^f = 1$ and such that $P(\tilde{t}) = 1/2$ for $\tilde{t} = 60$ fs; see Eq. (18). The initial relative phase is $\Phi^i = 0$ and the target phase is $\Phi^f = \pi/2$. A quadratic polynomial is chosen for the relative phase such that $\Phi(t_0) = \Phi^i$, $\Phi(t_f) = \Phi^f$, and $\dot{\Phi}(\tilde{t}) = 0$. (a) Levels population dynamics along with $P(t)$; (b) relative phase dynamics $\phi(t)$ (continuous line) compared to the chosen dynamics function $\Phi(t)$ (dotted line with points); (c) applied electric field, Eq. (13), and (d) detuning from the resonance frequency $\dot{\Phi}(t) + \dot{\Lambda}(t)$.

selected $\alpha = 0.068$ fs^{-1} and $\tilde{t} = 60$ fs. From panels (a) and (b), we note that the population and the relative phase follows the prescribed dynamical functions. Panels (a) to (c) show that up to $t = 40$ fs the field acts to change the relative phase and only then starts to effectively change the populations. The detuning shown in panel (d) has a marked depression around $t = 45$ fs combined with an overall decrease.

In the previous applications, the pulses generated by the dynamical functions have the inconvenience of abrupt turning on and turning off. In order to design a smooth switch on and off of the pulses, we must choose both $\dot{P}(t)$ and $\dot{\Phi}(t)$ close to zero at t_0 and t_f and with slow increasing or decreasing around these times. In order to illustrate this scenario, we chose for $\Phi(t)$ the following functional form which combines two hyperbolic secant functions:

$$\Phi(t) = \begin{cases} \chi_1 \text{sech}[\eta_1(t - \tilde{t})] + \sigma_1, & \text{if} \quad t < \tilde{t}, \\ \chi_2 \text{sech}[\eta_2(t - \tilde{t})] + \sigma_2, & \text{if} \quad t \geqslant \tilde{t}, \end{cases} \tag{19}$$

where $\chi_1 = (\Phi^{\max} - \Phi^i)/[\text{sech}(\eta_1 \tilde{t}) - 1]$, $\chi_2 = (\Phi^{\max} - \Phi^f)/\{\text{sech}[\eta_1(t_f - \tilde{t})] - 1\}$, $\sigma_1 = \Phi^{\max} - \chi_1$, and $\sigma_2 = \Phi^{\max} - \chi_2$. The parameters η_1 and $\Phi^{\max}$ as well as $\tilde{t}$ are freely chosen. $\Phi^{\max}$ sets the maximum value of $\Phi(t)$ at $t = \tilde{t}$, while η_1 relates to how fast this maximum is approached from the left. Furthermore, the relation $\eta_2 = \eta_1 \sqrt{\chi_1/\chi_2}$ guarantees the continuity of the second derivative of $\Phi(t)$ at $t = \tilde{t}$. Figure 6 presents the results with this choice of Eq. (19) for the dynamical function $\Phi(t)$ and Eq. (18) for $P(t)$. We have selected $P^i = 0.99$ and $P^f = 0.01$, while $\alpha = 0.04$ fs^{-1}, $t_f = 200$ fs, and $\tilde{t} = 100$ fs. For the relative phase, we choose $\Phi^i = 0$ and $\Phi^f = \pi/4$. Note that the chosen values for P_i and P_f avoid the extrema. The reason is that we must have $\dot{P}(t) = 0$ whenever $P(t) = 0$ or $P(t) = 1$, but the hyperbolic tangent function cannot strictly satisfy this condition for finite times. The parameters in Eq. (19) have been set to $\Phi^{\max} = 1.4\Phi^f$ and $\eta_1 = 1.65\alpha$. Panels (a) and (b) shows that the population and relative phase follow the prescribed dynamics. Panel (c) shows that the control pulse has the desired bell-shaped envelope. Panel (d) shows that the detuning has a change in sign around the peak of the pulse.

Finally, we return to the problem of having the same initial and final populations but with distinct initial and final relative phase. As seen before, it is not possible to keep the populations constant during the whole time interval if they are equal or very close to 1/2, while changing the relative phase. However, it is possible to set $P^i = P^f = 1/2$, without $P(t)$ being a constant. We address this situation by choosing the hyperbolic secant function for $P(t)$,

$$P(t) = G \,\text{sech}[\eta(t - t_p)] + F, \tag{20}$$

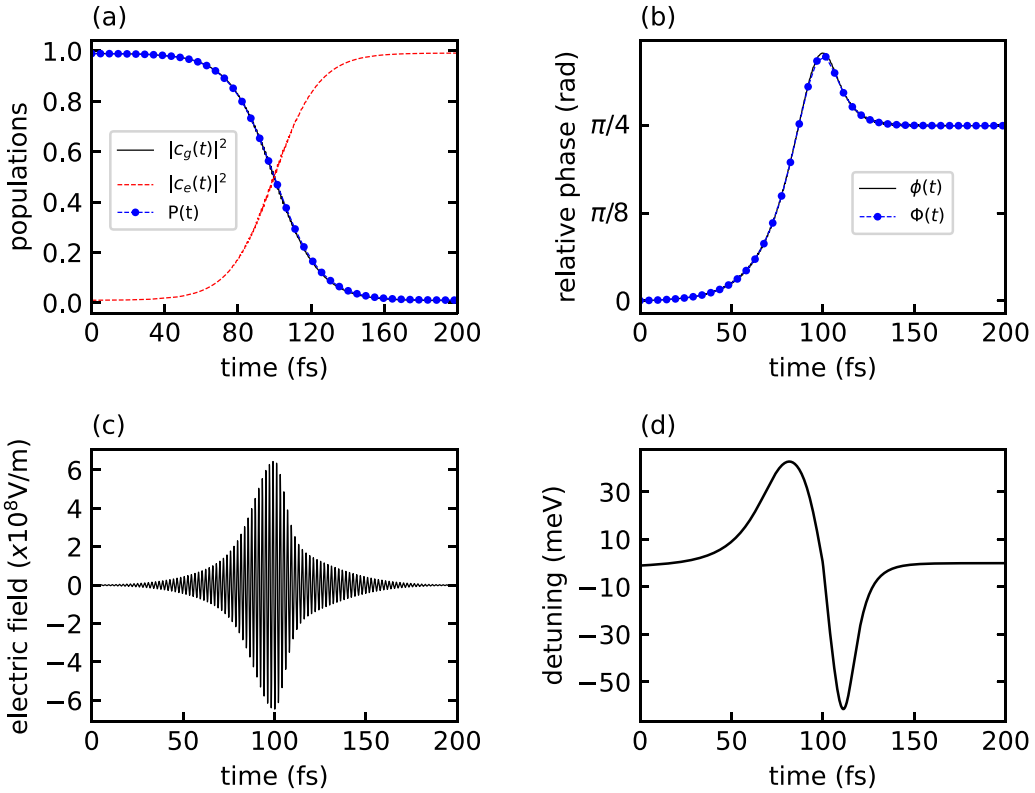

FIG. 6. $P(t)$ is a hyperbolic tangent function joining asymptotically $P^i = 0.99$ to $P^f = 0.01$ and such that $P(\tilde{t}) = 1/2$ for $\tilde{t} = 100$ fs; see Eq. (18). The initial relative phase is $\Phi^i = 0$ and the target phase is $\Phi^f = \pi/4$. A hyperbolic secant function is chosen for the relative phase such that $\Phi(t_0) = \Phi^i$, $\Phi(t_f) = \Phi^f$, and $\dot{\Phi}(\tilde{t}) = 0$; see Eq. (19). (a) Levels population dynamics along with $P(t)$; (b) relative phase dynamics $\phi(t)$ (continuous line) compared to the chosen dynamics function $\Phi(t)$ (dotted line with points); (c) applied electric field, Eq. (13), and (d) detuning from the resonance frequency $\dot{\Phi}(t) + \dot{\Lambda}(t)$.

where $G = P^{\max} - P^i$, $F = P^i$, and with $t_p = (t_f - t_0)/2$. The parameter η sets how sharp the function is, while $P^{\max} = P(t_p)$ defines its maximum or minimum value, which can be arbitrarily chosen in the interval $0 < P^{\max} < 1$, except for $1/2$. Thus the function $P(t)$ connects the same initial and final values. Note that since we will set $P^i = P^f = 1/2$, the time derivative of $\Phi(t)$ does not need to vanish in the interval $t_0 < t < t_f$. Therefore, we select a hyperbolic tangent function for $\Phi(t)$ joining asymptotically Φ^i to Φ^f,

$$\Phi(t) = R \tanh[\xi(t - t^*)] + S, \tag{21}$$

where $R = (\Phi^f - \Phi^i)/2$ and $S = (\Phi^f + \Phi^i)/2$. The parameter ξ controls the transition time between the initial and final relative phase and t^* is such that $\Phi(t^*) = S$. We set $t^* = t_p$, which produces a pulse with an apparent symmetry around t_p. Figure 7 illustrates the application of this scheme with the following set of parameters: $\Phi^i = 0$, $\Phi^f = \pi/8$, $P^{\max} = 0.7$, $t_f = 200$ fs, $t_p = t_f/2$, and $\eta = \xi = 0.08$ fs^{-1}. As in the previous cases, panels (a) and (b) show that the dynamics follows the prescribed dynamical functions. The envelope of the generated field in panel (c) has the expected bell shape with a small plateau around $t = t_p$. The detuning presented in panel (d) indicates that the modulation of the frequency of the control field consists of adding a constant frequency to ω_0; then there occurs an abrupt change around the time of the transition to a new constant frequency.

IV. CONCLUSION

In this work, we have derived an analytic expression for the external field acting on a two-level quantum system aimed at controlling simultaneously the population and the relative phase dynamics. The control field is engineered from two user-defined dynamical functions $P(t)$ and $\Phi(t)$ which join initial conditions to the target values. These functions must satisfy a series of conditions, but there is still great flexibility in their choices. It is worth emphasizing that the obtained expression can be easily built, needing, apart from the dynamical function themselves, only their derivatives. We have applied our approach to several initial and target values of population and relative phase, utilizing different dynamical functions. Although the obtained fields may not be experimentally accessible at the present, due, for instance, to high chirp rates [40,41], our calculations demonstrate the general applicability of the approach, with the only essential limitation being the validity of the RWA. We expect the present result to be used beyond the simple two-level system, e.g., in the strong-field control and for the control of many-level molecular systems [39,42]. In particular, our

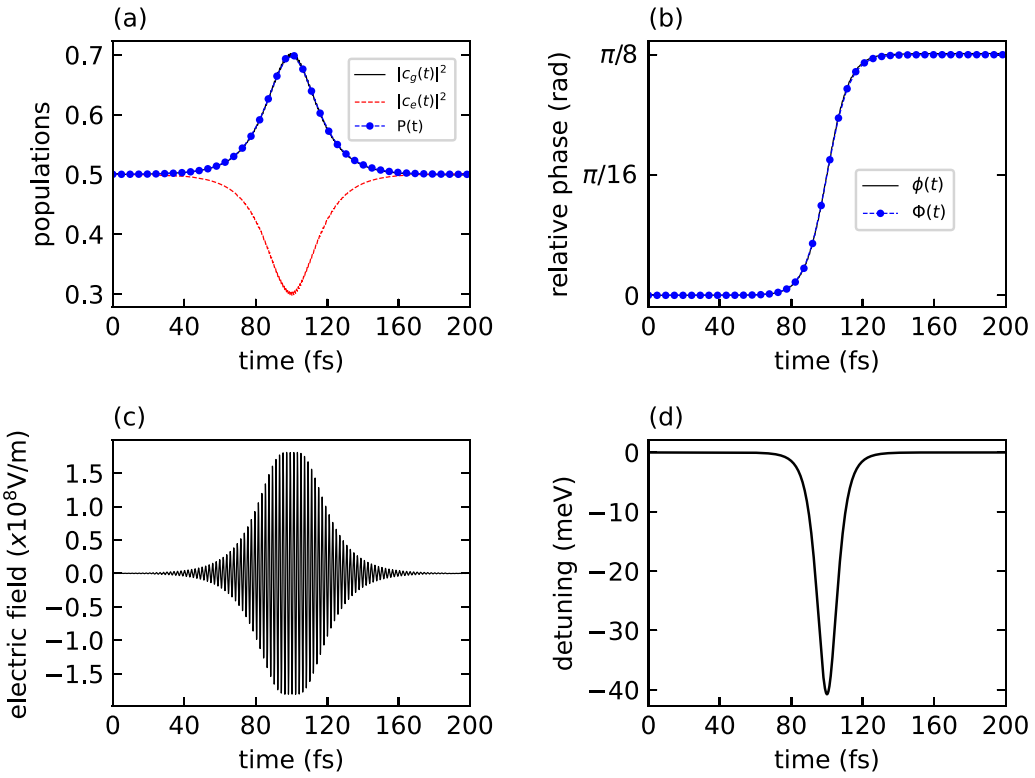

FIG. 7. $P(t)$ is a hyperbolic secant function joining asymptotically $P^i = 0.5$ to $P^f = 0.5$ and such that $P^{\max} = 0.7$ for $t_p = 100$ fs; see Eq. (20). The initial relative phase is $\Phi^i = 0$ and the target phase is $\Phi^f = \pi/8$. A hyperbolic tangent function is chosen for the relative phase joining asymptotically Φ^i to Φ^f and such that $\Phi(t_p) = (\Phi^f - \Phi^i)/2$; see Eq. (21). (a) Levels population dynamics along with $P(t)$; (b) relative phase dynamics $\phi(t)$ (continuous line) compared to the chosen dynamics function $\Phi(t)$ (dotted line with points); (c) applied electric field, Eq. (13), and (d) detuning from the resonance frequency $\dot{\Phi}(t) + \dot{\Lambda}(t)$.

scheme can be applied to engineer external fields to generate Rabi oscillations in atomic systems, which is currently attracting great interest [43,44]. Finally, the robustness of the engineered fields with respect to perturbations in the values of the system parameters should be considered in future works, as it is important for practical applications of the present methodology.

ACKNOWLEDGMENTS

E.F.L. acknowledges support from the Brazilian agency São Paulo Research Foundation, FAPESP (Grants No. 2023/04930-4 and No. 2014/23648-9). F.S.F. and E.F.L. acknowledge support from the National Council for Scientific and Technological Development–CNPq-Brazil through the PIBIC-Scholarship 2023-2024.

[1] D. X. Li and X. Q. Shao, Rapid population transfer of a two-level system by a polychromatic driving field, Sci. Rep. **9**, 9023 (2019).

[2] A. Migliore and A. Messina, Controlling the charge-transfer dynamics of two-level systems around avoided crossings, J. Chem. Phys. **160**, 084112 (2024).

[3] T. Hönigl-Decrinis, R. Shaikhaidarov, S. E. de Graaf, V. N. Antonov, and O. V. Astafiev, Two-level system as a quantum sensor for absolute calibration of power, Phys. Rev. Appl. **13**, 024066 (2020).

[4] J. C. L. Carreño, C. Sánchez Muñoz, E. del Valle, and F. P. Laussy, Excitation with quantum light. II. Exciting a two-level system, Phys. Rev. A **94**, 063826 (2016).

[5] L. Allen and J. H. Eberly, *Optical Resonance and Two-Level Atoms* (Dover Publications, Mineola, NY, 1987).

[6] C. H. Bennett and D. P. DiVincenzo, Quantum information and computation, Nature (London) **404**, 247 (2000).

[7] C. M. Tesch and R. de Vivie-Riedle, Vibrational molecular quantum computing basis set independence and theoretical realization of the Deutsch-Jozsa algorithm, J. Chem. Phys. **121**, 12158 (2004).

[8] K. Mishima and K. Yamashita, Quantum computing using molecular vibrational and rotational modes of the open-shell ^{14}N ^{16}O molecule, Chem. Phys. **367**, 63 (2010).

[9] E. Barnes and S. Das Sarma, Analytically solvable driven time-dependent two-level quantum systems, Phys. Rev. Lett. **109**, 060401 (2012).

[10] H. Liang, Generating arbitrary analytically solvable two-level systems, J. Phys. A: Math. Theor. **57**, 095301 (2024).

[11] A. Gangopadhyay, M. Dzero, and V. Galitski, Exact solution for quantum dynamics of a periodically driven two-level system, Phys. Rev. B **82**, 024303 (2010).

[12] I. I. Rabi, Space quantization in a gyrating magnetic field, Phys. Rev. **51**, 652 (1937).

[13] C. Zener and R. H. Fowler, Non-adiabatic crossing of energy levels, Proc. R. Soc. London, Ser. A **137**, 696 (1932).

[14] F. Peyraut, F. Holweck, and S. Guérin, Quantum control by few-cycles pulses: The two-level problem, Entropy **25**, 212 (2023).

[15] B. Amstrup, A. Lorincz, and S. A. Rice, Population inversion in a multilevel system: a model study, J. Phys. Chem. **97**, 6175 (1993).

[16] J. Cao, C. J. Bardeen, and K. R. Wilson, Molecular π pulses: Population inversion with positively chirped short pulses, J. Chem. Phys. **113**, 1898 (2000).

[17] J. Cao, C. J. Bardeen, and K. R. Wilson, Molecular "π pulse" for total inversion of electronic state population, Phys. Rev. Lett. **80**, 1406 (1998).

[18] I. I. Beterov, D. B. Tretyakov, V. M. Entin, E. A. Yakshina, I. I. Ryabtsev, M. Saffman, and S. Bergamini, Application of adiabatic passage in Rydberg atomic ensembles for quantum information processing, J. Phys. B: At., Mol., Opt. Phys. **53**, 182001 (2020).

[19] M. Demirplak and S. A. Rice, Adiabatic population transfer with control fields, J. Phys. Chem. A **107**, 9937 (2003).

[20] S. Shi and H. Rabitz, Quantum mechanical optimal control of physical observables in microsystems, J. Chem. Phys. **92**, 364 (1990).

[21] G. Dridi, K. Liu, and S. Guérin, Optimal robust quantum control by inverse geometric optimization, Phys. Rev. Lett. **125**, 250403 (2020).

[22] M. Shapiro and P. Brumer, Optimal control theory, in *Quantum Control of Molecular Processes* (John Wiley & Sons, Ltd, New York, 2011), Chap. 5, pp. 83–94.

[23] L. Shen and H. Rabitz, Optimal control of vibronic population inversion with inclusion of molecular rotation, J. Chem. Phys. **100**, 4811 (1994).

[24] Q. Zhang, X. Chen, and D. Guéry-Odelin, Reverse engineering protocols for controlling spin dynamics, Sci. Rep. **7**, 15814 (2017).

[25] S. González-Resines, D. Guéry-Odelin, A. Tobalina, I. Lizuain, E. Torrontegui, and J. G. Muga, Invariant-based inverse engineering of crane control parameters, Phys. Rev. Appl. **8**, 054008 (2017).

[26] M. Z. Wang, W. Ma, and S. L. Wu, Steady state engineering of a two-level system by the mixed-state inverse engineering scheme, Sci. Rep. **14**, 3409 (2024).

[27] N. V. Vitanov and B. W. Shore, Designer evolution of quantum systems by inverse engineering, J. Phys. B: At., Mol., Opt. Phys. **48**, 174008 (2015).

[28] M. Mirrahimi, G. Turinici, and P. Rouchon, Reference trajectory tracking for locally designed coherent quantum controls, J. Phys. Chem. A **109**, 2631 (2005).

[29] A. B. Magann, T.-S. Ho, C. Arenz, and H. A. Rabitz, Quantum tracking control of the orientation of symmetric-top molecules, Phys. Rev. A **108**, 033106 (2023).

[30] A. Magann, T.-S. Ho, and H. Rabitz, Singularity-free quantum tracking control of molecular rotor orientation, Phys. Rev. A **98**, 043429 (2018).

[31] Y. Chen, P. Gross, V. Ramakrishna, H. Rabitz, K. Mease, and H. Singh, Control of classical regime molecular objectives—applications of tracking and variations on the theme, Automatica **33**, 1617 (1997).

[32] P. Gross, H. Singh, H. Rabitz, K. Mease, and G. M. Huang, Inverse quantum-mechanical control: A means for design and a test of intuition, Phys. Rev. A **47**, 4593 (1993).

[33] N. V. Golubev and A. I. Kuleff, Control of populations of two-level systems by a single resonant laser pulse, Phys. Rev. A **90**, 035401 (2014).

[34] D. Ran, W.-J. Shan, Z.-C. Shi, Z.-B. Yang, J. Song, and Y. Xia, Pulse reverse engineering for controlling two-level quantum systems, Phys. Rev. A **101**, 023822 (2020).

[35] S. Grira, N. Boutabba, and H. Eleuch, Atomic population inversion in a two-level atom for shaped and chirped laser pulses: Exact solutions of Bloch equations with dephasing, Results Phys. **26**, 104419 (2021).

[36] I. Medina and F. L. Semião, Pulse engineering for population control under dephasing and dissipation, Phys. Rev. A **100**, 012103 (2019).

[37] A. Csehi, Control of the populations and phases of two-level quantum systems by a single frequency-chirped laser pulse, J. Phys. B: At., Mol., Opt. Phys. **52**, 195004 (2019).

[38] N. V. Golubev and A. I. Kuleff, Control of charge migration in molecules by ultrashort laser pulses, Phys. Rev. A **91**, 051401(R) (2015).

[39] L. Biró and A. Csehi, Coherent control of the vibrational dynamics of aligned heteronuclear diatomic molecules, Phys. Rev. A **106**, 043113 (2022).

[40] P. J. Delfyett, D. Mandridis, M. U. Piracha, D. Nguyen, K. Kim, and S. Lee, Chirped pulse laser sources and applications, Prog. Quantum Electron. **36**, 475 (2012).

[41] B. Kaufman, T. Paltoo, T. Grogan, T. Pena, J. P. S. John, and M. J. Wright, Pulsed, controlled, frequency-chirped laser light at GHz detunings for atomic physics experiments, Appl. Phys. B **123**, 58 (2017).

[42] A. Tóth and A. Csehi, Strong-field control by reverse engineering, Phys. Rev. A **104**, 063102 (2021).

[43] S. Nandi, E. Olofsson, M. Bertolino, S. Carlström, F. Zapata, D. Busto, C. Callegari, M. Di Fraia, P. Eng-Johnsson, R. Feifel, G. Gallician, M. Gisselbrecht, S. Maclot, L. Neoričić, J. Peschel, O. Plekan, K. C. Prince, R. J. Squibb, S. Zhong, P. V. Demekhin *et al.*, Observation of Rabi dynamics with a short-wavelength free-electron laser, Nature (London) **608**, 488 (2022).

[44] B. Tóth, A. Tóth, and A. Csehi, Competition of multiphoton ionization pathways in lithium, J. Phys. B: At. Mol. Opt. Phys. **57**, 055002 (2024).